Highly Ordered Thin Films of Octasubstituted Phthalocyanines

Paul Smolenyak,[†] Rebecca Peterson,[†] Ken Nebesny,[†] Michael Törker,[‡] David F. O'Brien,*[,†] and Neal R. Armstrong*[,†]

Contribution from the Department of Chemistry, University of Arizona, Tucson, Arizona 85721, and Institute für Angewandte Photophysik, Technical Universität Dresden, Dresden, Germany

Received May 6, 1999

Abstract: Phthalocyanines (Pc) modified at eight positions with benzyloxyethoxy groups ($CuPc(OC_2OBz)_8$ and $H_2Pc(OC_2OBz)_8$) form discotic mesophases in the bulk and self-assemble into cofacial rodlike aggregates in monolayers. These Pc aggregates form close packed arrays which are simple to process into highly coherent multilayer thin films. When these self-organizing molecular systems are compressed on the surface of an LB trough, the Pc columns align parallel to the compression barriers and form a rigid bilayer film (ca. 5.6 nm thick). Sections of these bilayer films can be mechanically removed from the trough surface with complete retention of integrity of the remaining film. This unprecedented behavior appears to arise from the multiple $\pi-\pi$ interactions between adjacent Pcs, resulting in unusually strong noncovalent interactions. AFM and STM studies of monolayer and bilayer films show that they consist of Pc columns which are coherent over distances of 50−100 nm. Thin films consisting of up to 15 bilayers (ca. 84 nm) can be quickly built by a "mechanical stamping" process, and small-angle X-ray scattering characterization of these film materials confirms their unusual coherence. Large electrical and optical anisotropies are observed in multilayer films of $CuPc(OC_2OBz)_8$ and $H_2Pc(OC_2OBz)_8$ which are comparable to those previously reported for thin film assemblies based on side-chain-modified silicon phthalocyanine polymers.

Introduction

Molecules which form discotic mesophases with significant long-range order and anisotropic electrical and optical properties continue to be sought for applications in electrical or optical logic circuits, electroluminescence devices, and electrochromic displays, among others.[1−16] Side-chain-modified phthalocyanines form a major class of discotic mesophase materials, and there are multiple examples of these molecules which aggregate or polymerize into rodlike assemblies with extremely interesting optical and electrical properties. Tailoring conductivity, optical band gap, luminescence energy and efficiency in thin films and "fibers" of these materials, through changes in their composition and molecular architecture, has been widely demonstrated.[1,6,8−10,14] Ordered organic thin films of these materials can often show large anisotropies in these properties,[1,2,5,8−10] which might be their most important advantage, if simple processing conditions can sustain these anisotropies in the macroscopic material.

Highly ordered thin films have been previously created using prepolymerized silicon phthalocyanines (PcPS), modified at either the 4 or 8 positions on each Pc with solubilizing side chains, forming rodlike units, each unit containing up to 100 Pcs.[1−5] These polymeric rods pack with excellent uniformity in orientation, parallel to the vertical dipping direction used for Langmuir−Blodgett thin film fabrication, and their large optical and electrical anisotropies form the basis for comparison of these properties in the materials reported here.

The disk-shaped monomeric 2,3,9,10,16,17,23,24-octakis(2-benzyloxyethoxy)phthalocyaninato copper, and its metal free analogue ($CuPc(OC_2OBz)_8$ and $H_2Pc(OC_2OBz)_8$ (Figure 1)), have recently been shown to exhibit a discotic mesophase in the bulk material, and a unique degree of self-assembly into coherent rodlike structures on the Langmuir trough.[12,13] Although many different side-chain-modified Pcs and other discotic molecules have been synthesized, few of these side chains have been terminated with aromatic functionality, and for those that have, the thin film properties either were not reported or did not show the properties of the Pcs reported here.[10,15,16] We are aware of only one other monomeric side-chain-modified Pc (possessing chiral centers in the side chain),[8]

* To whom correspondence should be addressed. E-mail: nra@u.arizona.edu; dfobrien@u.arizona.edu.
† University of Arizona.
‡ Technical Universität Dresden.

(1) Wegner, G. *Mol. Cryst. Liq. Cryst.* **1993**, *235*, 1.
(2) Sauer, T.; Arndt, T.; Batchelder, D. N.; Kalachev, A. A.; Wegner, G. *Thin Solid Films* **1990**, *187*, 357
(3) Wu, J. H.; Lieser, G.; Wegner, G. *Adv. Mater.* **1996**, *8*, 151.
(4) Ries, R.; Lieser, G.; Schwiegk, S.; Wegner, G. *Acta Polym.* **1997**, *48*, 536.
(5) Šilerová, R.; Kalvoda, L.; Neher, D.; Ferencz, A.; Wu, J.; Wegner, G. *Chem. Mater.* **1998**, *10*, 2284.
(6) Simon, J.; Bassoul, P. In *Phthalocyanines: Properties and Applications*; Lezneff, A. B. P., Ed.; VCH Publishers, Inc.: New York, 1993; Vol. 2, p 223.
(7) Toupance, T.; Bassoul, R.; Minear, L.; Simon, J. *J. Phys. Chem.* **1996**, *100*, 11704.
(8) van Nostrum, C. F.; Bosman, A. W.; Gelinck, G. H.; Schouten, P. G.; Warman, J. M.; Kentgens, P. M.; Devillers, M. A. C.; Meijerink, A.; Picken, S. J.; Sohling, U.; Shouten, A.-J.; Nolte, R. J. M. *Chem.—Eur. J.* **1995**, *1* (3), 171.
(9) Englekamp, H.; Meddelbeek, S.; Nolte, R. J. M. *Science* **1999**, *284*, 785.
(10) Fox, J. M.; Katz, T. J.; Van Elshocht, S.; Verbiest, T.; Kauranen, M.; Persoons, A.; Thongpanchang, T.; Krauss, T.; Brus, L. *J. Am. Chem. Soc.* **1999**, *121*, 3453.
(11) Cook, M. J. *J. Mater. Sci.: Mater. Electron.* **1994**, *5*, 117.
(12) Osburn, E. J.; Chau, L.-K.; Chen, S.-Y.; Collins, N.; O'Brien, D. F.; Armstrong, N. R. *Langmuir* **1996**, *12*, 4784.
(13) Smolenyak, P. E.; Osburn, E. J.; Chen, S.-Y.; Chau, L.-K.; O'Brien, D. F.; Armstrong, N. R. *Langmuir* **1997**, *13*, 6568.
(14) Osburn, E. J.; Schmidt, A.; Chau, L.-K.; Chen, S.-Y.; Smolenyak, P.; Armstrong, N. R.; O'Brien, D. F. *Adv. Mater.* **1996**, *8*, 926.
(15) Bryce, M. R. *J. Chem. Soc., Perkin Trans.* **1997**, *2*, 1671.

10.1021/ja991498b CCC: $18.00
Published on Web 09/03/1999

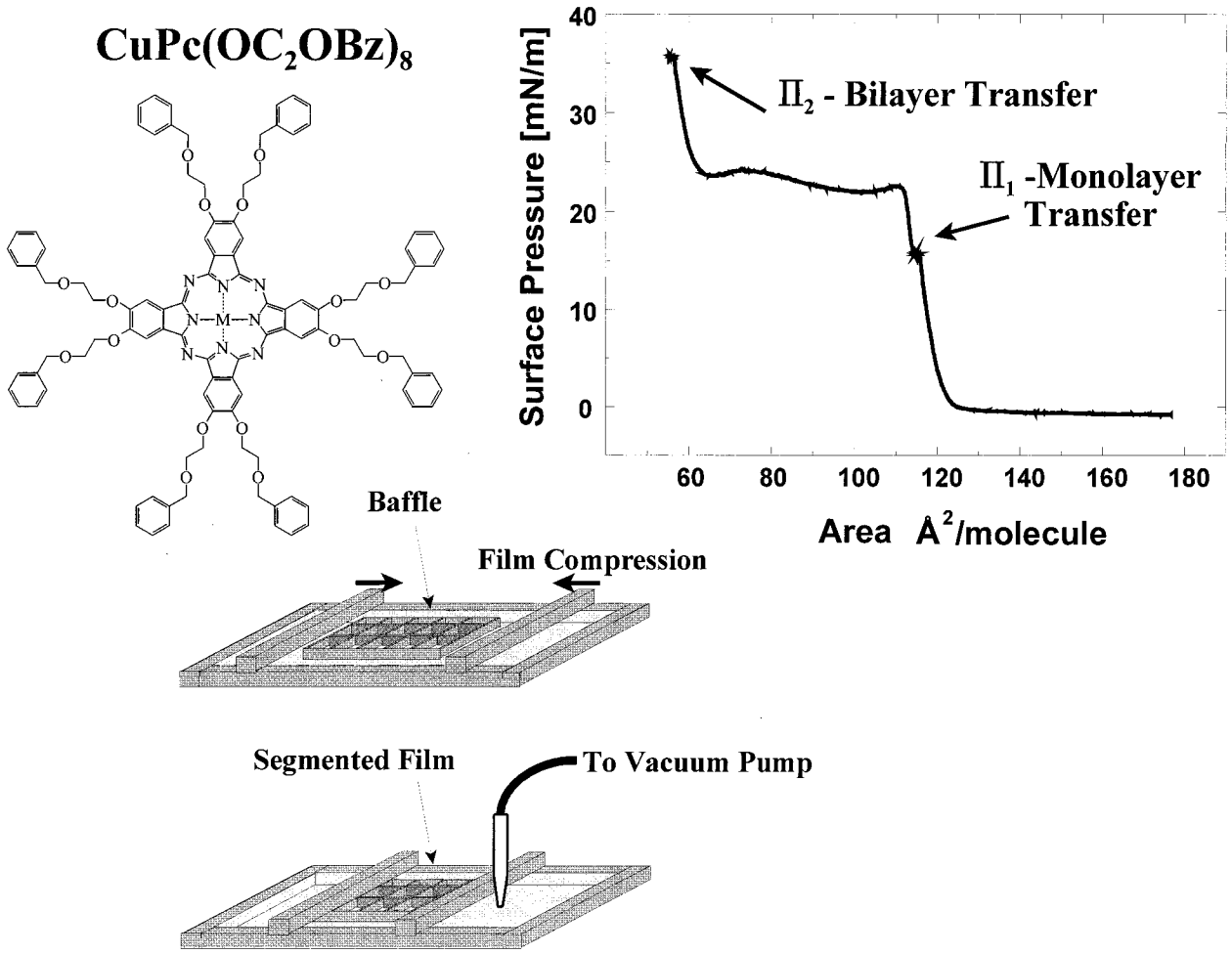

Figure 1. Pressure−area isotherm for $CuPc(OC_2OBz)_8$, showing the multiple phase transitions, and transfer pressures for creation of monolayer and bilayer films. Shown below the $\pi-A$ isotherm is the schematic view of the mechanical baffle system used to cut and stabilize the bilayer films into multiple rectangular sections, ready for horizontal transfer to various substrates.

which might produce the high degree of ordering in thin film formats that is reported here for the $CuPc(OC_2OBz)_8$ and $H_2Pc(OC_2OBz)_8$ systems. A recent report by Katz and co-workers also describes an unusual octaazaphthalocyanine which aggregates to form helical columnar structures with extremely large optical nonlinearities. The size of the aggregate structures in thin films of these materials, however, appeared to be less than 10 monomer Pc units per aggregate column.

The proper degree of film compression in the $CuPc(OC_2OBz)_8$ and the $H_2Pc(OC_2OBz)_8$ systems produces highly ordered bimolecular-layer thickness (bilayer) films with an unusual rigidity. The stability of the bilayer films leads to the new and simple deposition strategies described here, a type of "mechanical stamping" to quickly transfer bilayer sections of these films to various substrates, without sacrifice of the order achieved during film compression. This stamping process allows rapid formation of bilayer and multilayer thin film materials with coherence in structure along the Pc aggregate column axis, in each layer, of up to 70−100 nm, and coherence in the *z*-axis direction of multilayer films which suggest minimal defects in column−column packing, over distances up to 80 nm (the thickest films created so far). The multilayer films demonstrate optical and electrical anisotropies, comparable to those reported for multilayers of the prepolymerized PcPS assemblies. Reflectance FT-IR data for 1−3 bilayer coverage films on Au and X-ray scattering data for the fiber forms of these materials, both suggest that such coherent structures are obtained with tight cofacial packing of the Pc rings. The Pc rings are not perpendicular to the director axis of the rodlike column, as is the case for the polymerized silicon phthalocyanines. There is less order in the side chains of these aggregate assemblies than in the columns defined by the Pc cores, which may be a consequence of the need to minimize free space between the side chains and to create close packing in the multilayer and fiber forms of these materials.

Experimental Section

Molecules. (2,3,9,10,16,17,23,24-Octakis((2-benzyloxy)ethoxy)-phthalocayninato) copper and (2,3,9,10,16,17,23,24-Octakis((2-benzyloxy)ethoxy)phthalocayninato) dihydrogen were synthesized as reported by Osburn et al.[12] and Smolenyak et al.[13] Solutions of $CuPc(OC_2OBz)_8$ and $H_2Pc(OC_2OBz)_8$ were prepared using HPLC grade chloroform (Aldrich).

Substrates. Si(100) wafers (MEMC Electronic Materials, Inc.) were used for deposition of $CuPc(OC_2OBz)_8$ or $H_2Pc(OC_2OBz)_8$ bilayers and multilayers for AFM, X-ray reflectometry, and transmission FT-IR characterization. Before film deposition, these substrates were silanized with a 20% solution of 1,3-diphenyl-1,1,3,3-tetramethyldisilazane, 96% (Aldrich) in HPLC grade chloroform. Au (111) on mica substrates, used in the STM studies, were prepared by evaporating Au at ca. 3 Å/s onto a freshly cleaved mica substrate surface held at ca. 450 °C in a vacuum of ca. 10^{-7} Torr. LB films of $CuPc(OC_2OBz)_8$ or $H_2Pc(OC_2OBz)_8$ were deposited on the Au/mica substrates immediately after removal from vacuum. Au substrates, used in reflectance FT-IR studies, consisting of a ca. 1000 Å Au layer on a titanium-treated float glass were obtained from Evaporated Metal Films (Ithaca, NY). Au slides were cleaned by immersing in a 1:4 solution of H_2O_2/H_2SO_4 for 10 s

and then rinsing with water. Slides were modified by immersing in a 0.10 mM solution of benzyloxyethoxythiol, synthesized previously in this laboratory.[17] Modified substrates were washed with ethanol to remove unreacted thiols, dried in a stream of nitrogen, and stored in a sealed container.

Langmuir−Blodgett Materials and Techniques. Langmuir−Blodgett films were prepared on a Riegler & Kerstein RK3 LB trough. The trough was equipped with a Whilhemy balance (WS1) mounted midway between the compression barriers. The water subphase was purified using a Millipore Milli-Q system. Films were prepared by expanding the barriers completely, zeroing the balance, applying the material, letting solvent evaporate for 15 min, and compressing at 29.6 cm^2/s to a set pressure (see text). Langmuir films were subsequently lowered onto a baffle already beneath the air−water interface, partitioning the film into 15 separate rectangular isolated regions (see text and Figure 1).[17] Transfers were made using the horizontal or Schaefer transfer method.[18] A motor mounted above the trough drove the substrate into the film at ca. 0.15 cm/s, paused at the interface for 10 s, and lifted the film up at ca. 0.01 cm/s. Each bilayer transfer was done in a separate section of the baffle. Any remaining water left on the LB film after transfer was removed with dry nitrogen gas.

Scanning Tunneling and Atomic Force Microscopy. STM images were recorded on a Nanoscope III (Digital Instruments, Santa Barbara, CA), using mechanically cut Pt/Ir tips. The picoamp boost stage was set to 10^{10} V/A with 4 kHz filtering and the scanner was calibrated on a 5 nm × 5 nm scan of freshly cleaved HOPG. Images were obtained using bias potentials between ±10 and ±500 mV. All images were obtained in air on unannealed, but dry films, where no attempt had been made to remove water trapped in these films (see below).

AFM images were recorded in tapping mode, with the Nanoscope III system, with the sample immersed in pure water in the standard Digital Instruments solution cell. Oxide sharpened silicon nitride tips were used throughout. Images were obtained using cantilevers with nominal force constants of 0.58, 0.38, and 0.12 N/m; however, the best images were obtained with the "short thin" or 0.38 N/m cantilever. After ozone cleaning of the tip (see text) and immersion of the sample in solution, the entire system was allowed to equilibrate for 0.5−1.5 h before image acquisition. Cantilevers were tuned to resonant frequencies of ca. 29−32 kHz. Oscillation amplitudes of 0.3−0.4 V (ca. 8−10 nm) gave the best images. Tip forces were minimized after engagement by gradually lowering the tip onto the sample until proper tracking of the corrugated surface was evident, as observed both in the image and scope modes. Raw images were obtained in both height and amplitude mode, although the amplitude images showed the best contrast for display.

Low-Angle X-ray Reflectometry. Low-angle X-ray reflectometry measurements of 15 bilayer annealed and unannealed samples of $CuPc(OC_2OBz)_8$ and $H_2Pc(OC_2OBz)_8$ on Si(100) were obtained with a Kratos XRD-6000 instrument, with Cu(Kα) radiation and Bragg−Brentano optics, in collaboration with Dr. Simon Bates at Kratos Analytical.

Thin Film Conductivity. The dc conductivity of $CuPc(OC_2OBz)_8$ and $H_2Pc(OC_2OBz)_8$ thin films was determined after deposition on interdigitated array microelectrodes (IME) with ca. 15 μm spacing, 50 finger pairs per device (Abtech). Conductivity measurements were done in a vacuum (ca. 10^{-8} Torr) to minimize interference from adsorbed gases and adventitious water. Conductivity values were calculated from the current response of linear bias potential scans from 0 V to ±10 V. The Pc film on the IME was electrochemically doped by placing a drop of aqueous electrolyte (0.1M $LiClO_4$) over the area covered by the Pc file and inserting a Ag wire pseudoreference electrode and a Pt counter electrode into this solution drop. Pc films were poised potentiostatically at potentials sufficient to oxidize ca. 25% of the Pc rings within each film.[12,17] Following this electrochemical doping procedure, the electrolyte drop was removed from the surface while maintaining the Pc film under potential control, and the IME assembly was returned to the high vacuum environment for further conductivity measurements.

FT-IR Spectroscopy. FT-IR spectra were obtained with a dry-air purged Nicolet 550 spectrometer equipped with a tungsten source and MCT detector. A gold wire grid polarizer (Cambridge Physical Sciences) was used in the thin film transmission and RAIRS experiments. A film thickness of seven bilayers was used for transmission FT-IR of the Langmuir−Blodgett films. Annealed films were heated in air at 100 °C for 2 h. Two spectra were obtained for each sample: 0° and 90° polarization with substrate normal to incident beam. Blank spectra of the bare Si(100) substrates at the sample polarization and incident angles were taken for each sample prior to deposition. RAIRS spectra were obtained with an FT-80 Fixed 80° Grazing Angle Accessory (Spectra-Tech). One- and three-bilayer films were applied following surface modification by a self-assembled monolayer of benzyloxyethoxythiol. A blank spectrum was taken from a bare Au surface.

Results and Discussion

Pressure−Area Isotherms and Film Transfer. Aggregation of $CuPc(OC_2OBz)_8$ and $H_2Pc(OC_2OBz)_8$ occurs immediately upon deposition of the monomer-containing chloroform solutions onto the LB trough.[13] Compression of the thin film results in alignment and lengthening of the rodlike aggregate, with the Pc column axis parallel to the LB trough compression barriers (vide infra). The pressure−area isotherm for these materials (Figure 1) shows two distinct phase transitions which are assigned to the formation of a monolayer-thick film at Π_1 and a bilayer film at Π_2. Film compression−expansion studies indicate minimal hysteresis in the $\pi-A$ curve expansion curve, if compression is reversed at Π_1 and the film is allowed to expand back to the precompression trough area. Recompression of the film then generates an isotherm indistinguishable from the original. If the compression of these films proceeds to Π_2, however, considerable hysteresis is observed in the $\pi-A$ expansion curve and, as indicated by $\pi-A$ recompression curves, the bilayer film does not relax to its precompressed state. Continued compression of the $CuPc(OC_2OBz)_8$ and $H_2Pc(OC_2OBz)_8$ assemblies beyond Π_2 produces unusually robust fiber bundles (lengths of 1−10 cm) that can be removed intact from the subphase surface.[14] The Pc metal center strongly influences the self-assembly properties of these materials; for example, axial coordination of water by zinc inhibits formation of rigid monolayer or bilayer films or fibers of $ZnPc(OC_2OBz)_8$.[12]

Langmuir−Schaefer horizontal transfer methods are convenient for the transfer of rigid LB films to various substrates.[17,18] Horizontal transfer of $CuPc(OC_2OBz)_8$ and $H_2Pc(OC_2OBz)_8$ films to appropriately hydrophobized substrates allows the fabrication of bilayer films, resulting from single transfer events, at Π_2, at a surface pressure of ca. 35 mN/m (Figure 1). A unique feature associated with such horizontal transfers is that a stable hole is left behind in the film on the LB trough, with the shape of the substrate to which transfer was made, which does not disappear with continued compression of the film![13] These vacancies are stable at least up to 18 h, and several such vacancies can be created on these bilayer films, without loss of shape or collapse of the remaining film. These observations indicate an unusual stiffness of the thin film, due to strong noncovalent interactions between the Pc rings. These interactions create the possibility of repetitive transfer of ca. 5.6 nm thickness bilayer segments, without loss of film integrity or the need for recompression of the LB film.

Multilayer films are now prepared by taking advantage of this film stiffness and stability. After compression of $CuPc(OC_2OBz)_8$ or $H_2Pc(OC_2OBz)_8$ films to Π_2, compression is terminated and the water level in the subphase is slowly lowered

(16) Bryce, M. R. *Adv. Mater.* **1999**, *11*, 11.

(17) Smolenyak, P. E.; Peterson, R. A.; O'Brien, D. F.; Armstrong, N. R. *Porphyrins and Phthalocyanines*; John Wiley and Sons Ltd.: West Sussex, U.K., in press. Smolenyak, P. E. Ph.D. Dissertation, University of Arizona, 1998.

(18) Ulmann, A. *Ultrathin Organic Films*; Academic Press: New York, 1991; pp 127−129 and references therein.

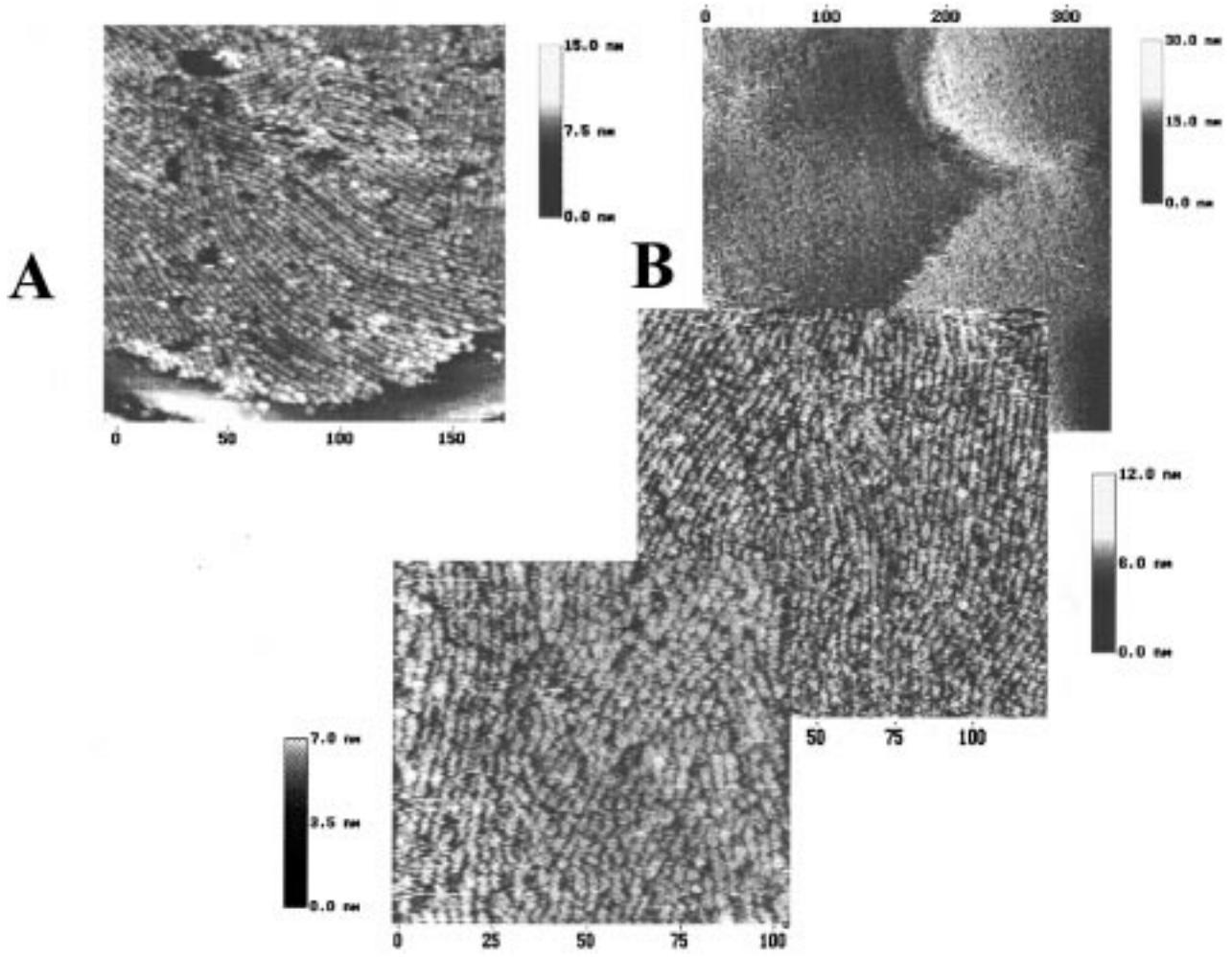

Figure 2. STM images of $CuPc(OC_2OBz)_8$ monolayer (A) and bilayer (B) films on Au(111)/mica substrates. The vertical axes in these images were parallel to the compression barrier direction. The horizontal axes indicate distance in nanometers.

until the entire compressed film (area = ca. 500 cm^2) contacts a metal baffle assembly (Figure 1). The baffle partitions cut the film into several stable bilayer sections, floating on their own small subphase regions, ready for horizontal transfer to the appropriate substrates. A modified dipping apparatus allows for rapid repositioning of the substrate holder over the center of each of these Pc film segments. Repetitive horizontal dipping cycles of hydrophobized glass and silicon(100) and alkanethiol-modified gold[19] transfers each segmented bilayer film with nearly 100% efficiency. Each dipping cycle picks up a Pc film with the rodlike Pc aggregates aligned with long axes parallel to the original compression barriers of the LB trough. The orientation of the substrate can be changed at the end of each dipping cycle, should it be desired to create thin films where the "director axis" of the Pc columns is angled with respect to the layer below or above it. If the compressed film is held at Π_1 (ca. 15 mN/m), single-molecule thickness films can be transferred to these same substrates by the horizontal dipping approach.

Imaging by Scanning Probe Microscopies. Parts A and B of Figure 2 are STM images of monolayer and bilayer $CuPc(OC_2OBz)_8$ films after horizontal transfer to a Au(111)/mica substrate. The films were allowed to dry after transfer, but were not annealed to remove the final traces of trapped water. In these monolayer and bilayer images, the STM data was obtained so that the vertical axis in the image is parallel to the compression barriers on the LB trough. Domains of densely packed Pc columns, each with ca. 5−10 columns per domain, are evident. The image of the $CuPc(OC_2OBz)_8$ monolayer shows coherence lengths of up to 75 nm for the Pc columns, and column−column spacings of ca. 2.8 nm, which is less than that expected if the Pc side chains were fully extended (ca. 3.4 nm). No particular orientation relative to the compression barriers dominates the monolayer film structure. Bilayer films show similar sized Pc domains, each with ca. 5−10 columns in close association, a column length of up to 75 nm, a column−column distance of 2.8−2.9 nm, like that seen in the monolayer films, but now the majority of Pc columns lie parallel to the axis defined by the compression barriers of the LB trough.

Tapping mode AFM images were obtained (in solution) of bilayer thick films (Figure 3) deposited by the horizontal dipping method on hydrophobized Si(100) substrates using silicon nitride tips. Structures and column alignments parallel to the LB trough compression barrier direction are observed, as for the STM data. Data collection parameters, however, occasionally required scanning at off-orthogonal angles for optimal imaging.

High-quality tapping mode AFM images of these materials could only be obtained by proper pretreatment of the AFM tips to make them as hydrophilic as possible. Figure 4 shows the force−distance curves at the Pc−water interface, where an as-received tip was used (Figure 4A) and where the tip was preconditioned in an ozone atmosphere, for periods up to 1 h, to completely remove hydrocarbon contamination (Figure 4B).

(19) Peterson, R. M.S. Thesis, University of Arizona, 1998.

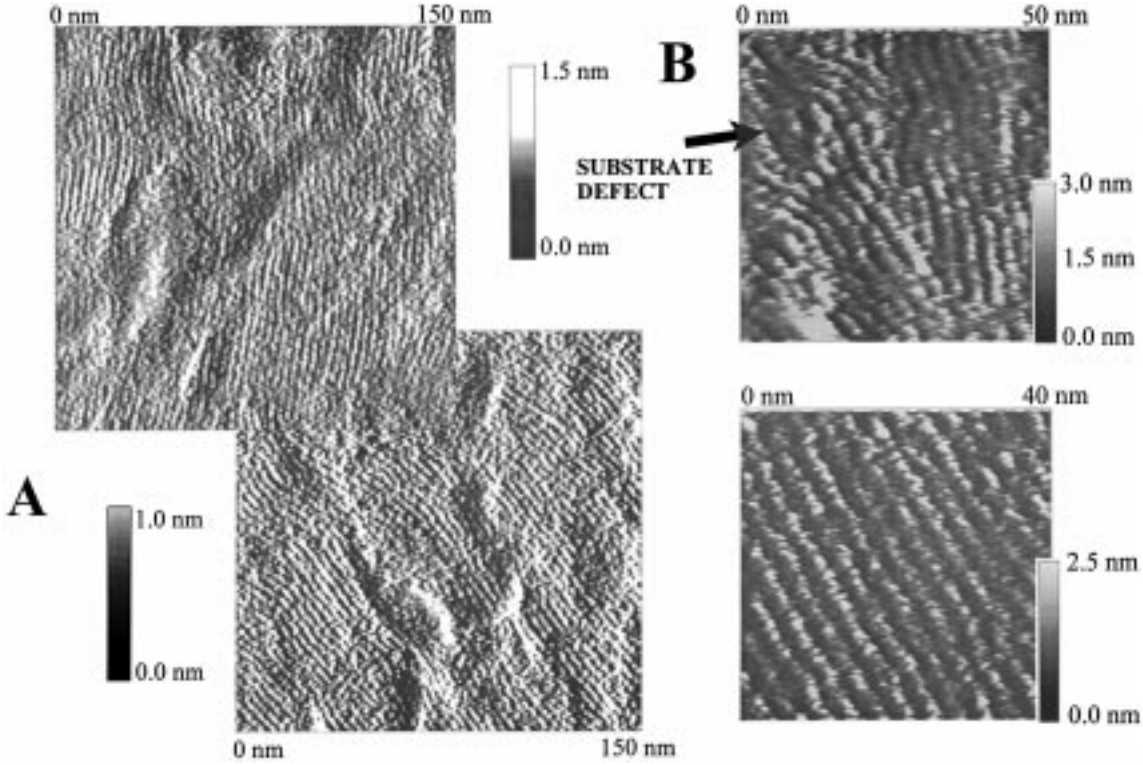

Figure 3. Tapping mode AFM images of $CuPc(OC_2OBz)_8$ bilayer films on hydrophobized Si(100) substrates, showing long-range columnar order and the ability to conform to variations in substrate topography. The images in (A) show two different views on the 150 nm × 150 nm scale, while the images in (B) are on the 50 nm × 50 nm and 40 nm × 40 nm scale, showing regions of column distortion and regions of column coherence, respectively.

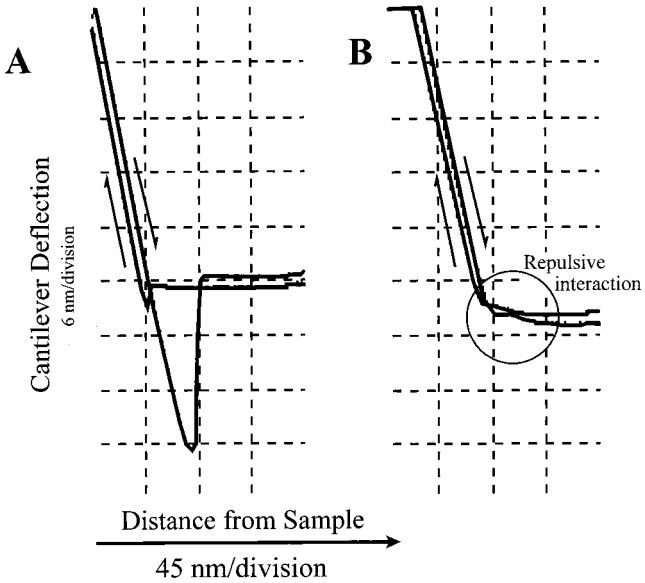

Figure 4. Force−distance curve for (A) the "as received" silicon nitride tapping mode AFM tips and (B) an ozone-treated tip, which had been made hydrophilic, and therefore exhibited a repulsive interaction with the Pc film surface.

Recent AFM studies of other soft and easily damaged materials suggest that proper imaging can only be obtained when the interactions between tip and sample are as repulsive as possible.[20] Tips which produced the force−distance curves of Figure 4A would occasionally allow for 1−2 nm lateral resolution imaging of the $CuPc(OC_2OBz)_8$ and $H_2Pc(OC_2OBz)_8$ thin films but would, over the space of a few minutes, lead to significant damage. Tips producing the force−distance curves of Figure 4B consistently produced good quality AFM images, with minimal sample damage.

In Figure 3A individual Pc columns show coherence over distances of 25−100 nm, even in regions of the thin film where the underlying substrate is not smooth. The average column−column spacing is ca. 2.9 nm. A feature observed in these images, which was not resolved in the STM studies, is the tendency for the Pc columns to conform to variations in substrate topography. Figure 3B shows a close-up of a region of good column order over a smooth substrate region (40 × 40 nm), and a comparable area where the Pc columns are forced to distort around a substrate defect (indicated by an arrow in the figure). It appears possible to "bend" these Pc columns by 15°−25°, over distances of ca. 10 nm, without complete disruption of the assembly.

We also find regions in these AFM images where the single bilayer is not complete, and single column-height "steps" can be resolved (Figure 5). Image detail in the lower layer is often lost at these steps, due to the rather sensitive optimization of tip−sample distance needed to provide nanometer resolution images. This lack of apparent order in the image of the lower layer is therefore only due to problems of maintaining optimal tip interactions with the Pc film, in this region. Bearing analysis of such a stepped region showed the step height to be ca. 2.9 nm, consistent with the column−column distance measured laterally. X-ray characterization of multilayer films (below) suggests a slightly smaller intercolumn lattice spacing and hexagonal packing of these columns, which should produce a step height near 2.4 nm. These partially completed bilayers may not assume purely hexagonal packing.

X-ray Reflectometry. Low-angle X-ray reflectometry of these films further confirms the long-range coherence of the deposited material and the improvement in ordering achieved

(20) Patrick, H. N.; Warr, G. G.; Manne S.; Aksay, I. A. *Langmuir* **1997**, *13*, 4349.

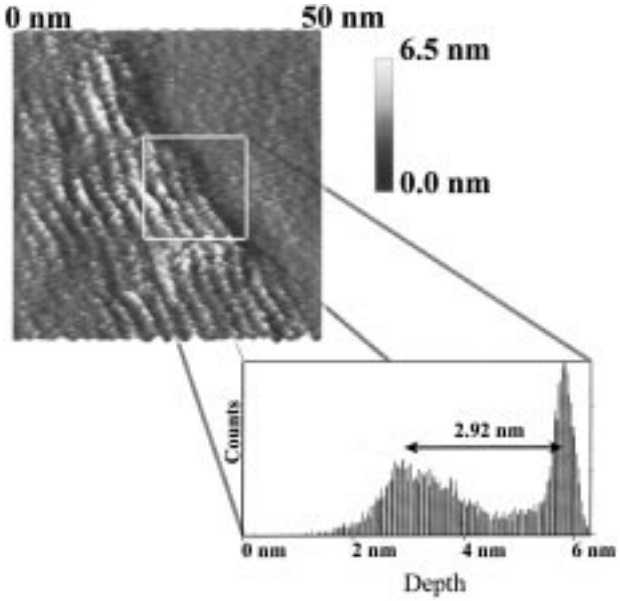

Figure 5. Tapping mode AFM image and bearing analysis of a region of a $H_2Pc(OC_2OBz)_8$ bilayer, where the second layer was not fully formed, and where a step-edge could be found.

with annealing (Figure 6). Single Bragg peaks at $2\theta = 3.75-3.79°$ were observed for all $CuPc(OC_2OBz)_8$ and $H_2Pc(OC_2OBz)_8$ multilayer films (30 monolayers, deposited as 15 separate bilayers, on hydrophobized Si(100)). This corresponds to a lattice parameter of $d = 2.33$ to 2.36 nm. Assuming hexagonal close packing, as suggested by wide-angle X-ray scattering (WAXS) characterization of fiberlike bundles of these same materials,[14] we find a Pc column−column distance of ca. 2.69−2.73 nm. As discussed below, this distance is consistent with Pc rings which sit at an angle to the column director axis, with some compression and reduced order in the substituent chain region of the columnar assemblies.

The full-width at half-maximum (fwhm) of the Bragg peaks in these X-ray data can be used to estimate coherence of the multilayer assembly in the *z*-axis direction, i.e., perpendicular to the substrate plane. The Scherrer relationship[21] allows for estimation of L, the coherence length in relation to $\Delta(2\theta)$, the fwhm of the Bragg reflection peak, and K, a constant, commonly assigned a value of 0.9, according to

$$L = \frac{\lambda K}{\cos\theta\ \Delta(2\theta)} \tag{1}$$

The $H_2Pc(OC_2OBz)_8$ films showed the largest fwhm in their unannealed state (0.449° in 2θ, coherence length = ca. 17.7 nm). With annealing in air at 100 °C for 2 h this fwhm decreased to ca. 0.223° in 2θ and gave an estimated coherence length of 35.6 nm. For the $CuPc(OC_2OBz)_8$ films, the unannealed versions (Figure 6A) gave a fwhm of 0.126° in 2θ, and the air-annealed versions (Figure 6B) gave a fwhm of 0.123° in 2θ. This corresponds to a *z*-axis coherence length of up to 65 nm. The Kiessig fringes which appeared in the annealed versions of the $CuPc(OC_2OBz)_8$ films (Figure 6B), another indication of their high film quality, allowed for an estimation of film thickness of 73.5 nm, close to that predicted for the thickness of the 15-bilayer close-packed columnar array. A second small Bragg peak at 1.92° in 2θ is observed in unannealed versions of these films (Figure 6A) and is absent after annealing. There is clearly a tendency for stable bilayers to form in the process of horizontal film transfer, which imparts an additional periodicity to these films, which is eliminated by the annealing process. Given the fact that water is entrapped in these films, as transferred (see below), and that these reflections disappear upon annealing, it is reasonable to assume that this bilayer periodicity arises from layers of water trapped between stable bilayers.

Anisotropy in Electrical Conductivity. The anisotropy in electrical properties is estimated from the differences in conductivity for multilayer versions of these columnar assemblies, deposited on interdigitated microcircuit electrodes (IMEs, Figure 7). As demonstrated recently for both vertically and horizontally transferred LB PcPS films, two IMEs were placed on a substrate such that each bilayer transfer produced an ensemble of Pc columns with the director axis either parallel or perpendicular to the fingers of the IME.[5] Provided that good electrical contact is made between the Pc film and the gold contacts, such an arrangement allows for a direct measurement of the ratio of conductivities, $\sigma_\perp/\sigma_{||}$, where $\sigma_\perp$ represents

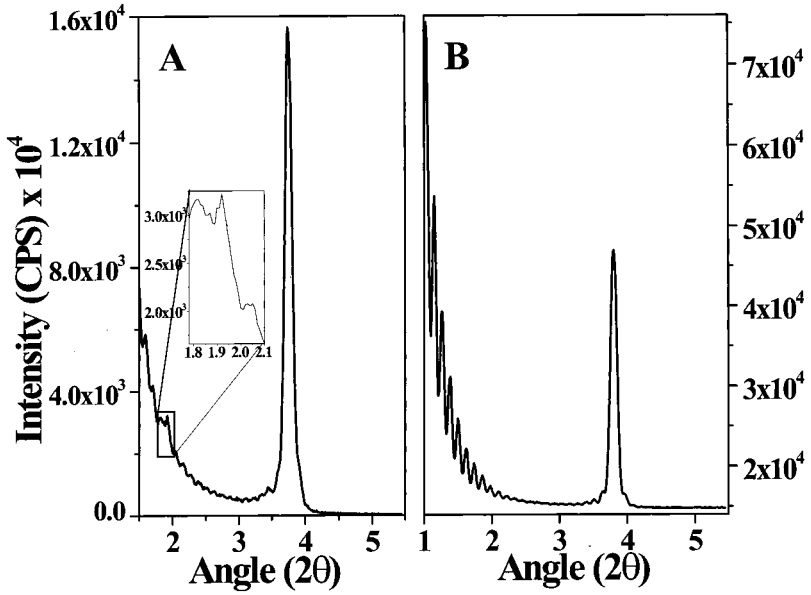

Figure 6. Small-angle X-ray scattering (SAXS) data for unannealed (A) and annealed (B) 30 monolayer films of $CuPc(OC_2OBz)_8$ on hydrophobized Si(100), showing the main Bragg peak at ca. 3.75°−3.79°corresponding to hcp lattice parameters of 2.33−2.36 nm and Pc-column−Pc-column distances of 2.69−2.73 nm.

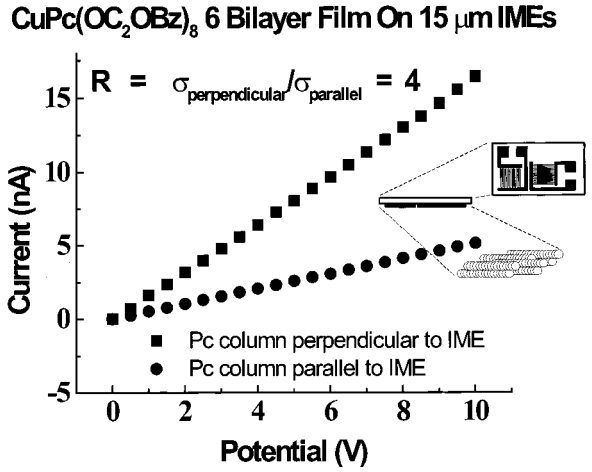

Figure 7. Current−voltage relationships for multilayer films of CuPc-$(OC_2OBz)_8$ on two different sets of interdigitated microcircuit electrode arrays (15 μm spacing) with two different orientations of the Pc columns, parallel and perpendicular to the contacting electrodes.

conductivity measured along the director axis of the Pc column (columns lying perpendicular to the IME fingers). For CuPc-$(OC_2OBz)_8$ and $H_2Pc(OC_2OBz)_8$ films over thicknesses from 4 to 15 bilayers, conductivities in the range 10^{-9}−10^{-8} Ω^{-1} cm^{-1} were observed, the ratio $\sigma_\perp/\sigma_{||}$ varied from 2.0 to 10.0, and a linear current−voltage response over potentials up to ca. 2.0 V was observed. These measurements were conducted with the thin film assemblies in high vacuum, after allowing for desorption of water from the thin film over the space of up to 1 h (as indicated by the signal from a mass spectrometer resident in the vacuum chamber). These current−voltage curves could be retraced multiple times, provided that voltages were not applied which exceeded those shown here (ca. 10 V). Electrochemical doping (of both annealed and unannealed films) by oxidation of ca. 25% of the Pc rings in these films in the presence of ClO_4^- anions,[17] typically raised the conductivities of the vacuum annealed Pc films by as much as a factor of 300, and did not change the $\sigma_\perp/\sigma_{||}$ ratio observed before doping. Furthermore, these electrochemically doped films sustained the higher levels of conductivity (ca. 10^{-6} to 10^{-5} Ω^{-1} cm^{-1}) for extended periods of time in a vacuum and upon return to atmospheric conditions. These conductivity values, however, are substantially below those observed for bulk versions of electrochemically doped crystalline (no side chains) polymeric silicon phthalocyanines of Marks and co-workers,[22,23] but comparable to those recently reported for PcPS thin films where the dc conductivity was measured with interdigitated array microelectrodes as was done here.[5] It is not known at present whether these lower conductivities are due to the inability for close approach of adjacent Pc columns, as in the silicon phthalocyanine polymers without side chains, or simply the lack of good electrical contacts to these Pc columnar assemblies.

There is a clear need to make good electrical contact between the aggregate chain ends of our Pc assemblies and the gold fingers on these electrode arrays. AFM characterization of the microcircuits, with and without the Pc films in place, indicated that the Pc films were effectively "cut" by the process of horizontal film transfer so that the Pc films fit between the gold fingers, where the surface of the Pc thin film was below the plane of the interdigitated microcircuit.[17] In this way, there is the potential for direct contact of a Pc aggregate rod with the side wall of a gold finger on the microcircuit, but no guarantee that this occurs. Therefore, the conductivity values reported here have to be considered a lower limit to the conductivity of individual Pc aggregate rods, and the variability in anisotropies must result from the variation in the quality of Pc-film/Au electrical contacts. The low values of $\sigma_\perp/\sigma_{||}$ are also not unexpected for Pc thin films with good columnar order over distances up to 50−100 nm but which are still not optimized to show this ordering over the distances required to span most of the space between gold fingers on the interdigitated array, i.e., conductivities and anisotropies in conductivities are still limited by movement of charge across defect sites in these thin films. Modification of all of the surfaces in the microcircuit to improve materials compatibility and electrical conductivity would appear to be essential, and these studies are in progress.

We have also recently measured the anisotropy of hole mobilities of $CuPc(OC_2OBz)_8$ thin films deposited as the channel region on silicon oxide gates, treating these materials as organic thin film transistors (OFETs).[24] Preliminary studies have not shown the saturation behavior expected of ideal OFET materials at high gate-source voltages. Hole mobilities in the range of 10^{-6} cm^2 V^{-1} s^{-1} were observed and were always at least a factor of 3 higher when measured along the Pc column axis direction, compared to mobilities measured perpendicular to the column axis. Further details of these studies, especially the affects of film processing on these mobilities, will be communicated later.

Microstructure within the Pc Columns. In-plane and out-of-plane infrared vibrational transitions in the Pc ring, and in the ethylene oxide side chains, were explored to provide additional insights into film order and the orientation of Pc rings with respect to the column director axis. We first discuss transmission experiments for multilayer films on Si(100), using two different polarizations of the incident beam for computing the absorbance intensity ratio ($A_\perp/A_{||}$) for vibrations which (a) lie in the plane of the Pc ring (ν_{Pc-O-C} for the alkoxy groups attached to the Pc ring (1204, 1283 cm^{-1}) and those in the ethylene oxide chains (ν_{C-O-C} 1103 cm^{-1})) and (b) for vibrations which occur out of the plane of the Pc ring (δ_{Pc-H} = 745 cm^{-1}).[17] The dichroism (Figure 8 and Table 1) in the δ_{Pc-H} out-of-plane bend is complimentary to the dichroism in the ν_{Pc-O-C} in-plane stretch and is consistent with the degree of dichroism noted most recently for the Q-band visible absorbance spectra of these Pc films.[13,15]

These transmission IR data lead to estimates of the order parameter S and an average tilt angle ψ, which describes the angle of the Pc ring with respect to the director axis of the Pc column.[2,17,19] The order parameter, S, is based on the intensity ratios of a specific vibration band using two orthogonally polarized beams and is related to the dichroic ratio $R = I_\perp/I_{||}$ by

$$S = \frac{R-1}{R+1}(1 - 2\cos^2\alpha) \qquad (2)$$

where α is the angle between a specific transition moment and the molecular symmetry axis. For the vibrations in and out of the plane of the Pc ring, $\alpha = 90°$ and 0°, respectively. Sauer et al. defined and determined the angle, ψ, which represents a deviation of PcPS columns away from the Langmuir−Blodgett

(21) Guinier, A. *X-ray Diffraction*; W. H. Freeman and Co.: San Francisco, 1963; pp 121−125.

(22) Gaudiello, J. G.; Kellogg, G. E.; Tetrick, S. M.; Marks, T. J. *J. Am. Chem. Soc.* **1989**, *111*, 5259.

(23) Almeida, M.; Gaudiello, J. G.; Kellog, G. E.; Tetrick, S. M.; Marcy, H. O.; McCarthy, W. J.; Butler, J. C.; Kannewurf, C. R.; Marks, T. J. *J. Am. Chem. Soc.* **1989**, *111*, 5271.

(24) Collaboration with Dr. Z. Bao, Lucent Technologies, AT&T Bell Laboratories; see also: Bao, Z.; Lovinger, A. J.; Dodabalpur, A. *Adv. Mater.* **1997**, *9*, 42.

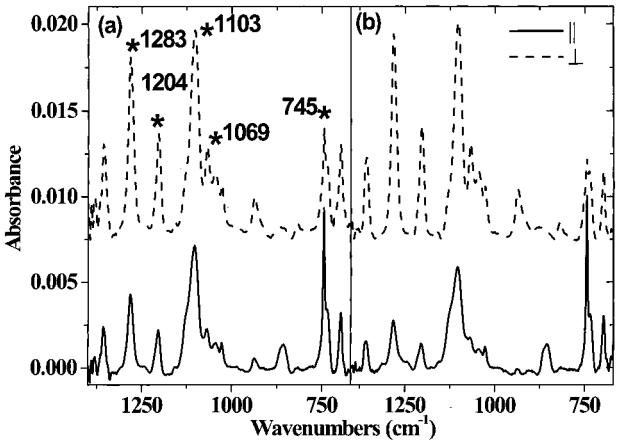

Figure 8. Transmission FT-IR data for seven bilayer films of unannealed (A) and annealed (B) films of $CuPc(OC_2OBz)_8$, showing the dichroic nature of these films (highlighted absorbance peaks were used in calculations shown in Tables 1 and 2).

Table 1. Transmission IR Data for 15-Bilayer $CuPc(OC_2OBz)_8$ Film on Si(100), Showing Dichroic Ratio (R), Order Parameter (S), and Tilt Angle (ψ) of the Pc with Respect to Column Director Axis, for Both In-Plane and Out-of-Plane Vibrations, before (rt) and after Annealing (100 °C, 2 h)

	before annealing			after annealing		
wavenumbers (cm^{-1})	R	S	ψ (deg)	R	S	ψ (deg)
745	0.70	0.18	39.8	0.46	0.37	34.3
1103	1.70	0.26	37.5	2.14	0.36	34.4
1204/1283	2.64	0.45	31.7	4.47	0.64	25.3

dipping axis, for various PcPs thin films.[2] Unlike the PcPS system, where the Pc molecules are polymerized to lie perpendicular to the main director axis, the phthalocyanine molecules of interest here are free to adopt a slip-stacked or angled stacking arrangement along the main director axis. We can still define a tilt angle, ψ, based on the interaction of a polarized electric field with a pair of orthogonal dipole moments in and out of the plane of the Pc core. The following relates the dichroic ratio, R, with ψ:

$$\langle \sin^2 \psi \rangle = \begin{cases} \dfrac{1}{R+1} & \text{for in plane modes} \\ \dfrac{R}{R+1} & \text{for out of plane modes} \end{cases} \quad (3)$$

For our Pc assemblies, we find that the values of S are strongly dependent upon the pretreatment of the Si(100) surface and the temperature at which film transfer from the LB trough was carried out.[17] The highest quality films were obtained in those cases where the Si(100) surface was pretreated with a phenyl-terminated silane (1,3-diphenyl-1,1,3,3,-tetramethyldisilazane) and where film transfer was carried out at trough temperatures near 0 °C. Values of S were always higher for the $CuPc(OC_2OBz)_8$ versus the $H_2Pc(OC_2OBz)_8$ films, and values of S increased for both systems upon annealing. The average value for ψ = ca. 30° determined from these measurements is consistent with the values determined from the reflection−absorption experiments described below.

Reflection−absorption FT-IR (RAIRS) characterization of multilayer films of $CuPc(OC_2OBz)_8$ and $H_2Pc(OC_2OBz)_8$, deposited on Au substrates using perpendicularly polarized incident radiation, was used to provide better estimates of the tilt angles of the Pc rings with respect to the substrate plane

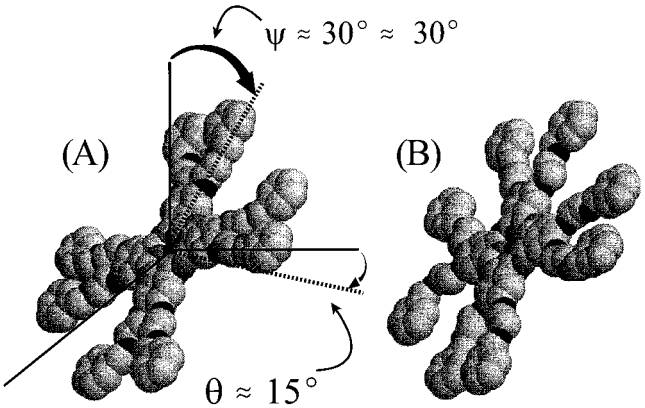

Figure 9. Schematic views of the inclination taken by individual Pcs in the $CuPc(OC_2OBz)_8$ columns, where ψ represents the angle of inclination of the plane of the Pc away from the surface normal (behind the plane of the page), and θ represents the twist of the plane of the Pc toward the reader. (a) represents the Pc with side chains fully extended, and (b) represents the same values of ψ and θ, but with distorted side chains.

Table 2. Calculated Euler Angles for One- and Three-Bilayer Coverages of $CuPc(OC_2OBz)_8$ and $H_2Pc(OC_2OBz)_8$ on a Au Surface, Previously Hydrophobized with an Alkanethiol Monolayer, Showing Average Angle of Inclination of the Pc Ring with Respect to the Surface Normal

		Euler angles for the Pc macrocycle plane		Euler angles for the Pc side chains	
	no. of bilayers	ψ_{RAIRS} (deg)	θ_{RAIRS} (deg)	ψ_{RAIRS} (deg)	θ_{RAIRS} (deg)
$CuPc(OC_2OBz)_8$	1	32.5	13.5	34.1	7.7
	3	30.2	19.4	33.2	17.9
$H_2Pc(OC_2OBz)_8$	1	23.9	15.7	32.8	11.7
	3	25.2	16.2	34.4	14.2

(Table 2).[25−27] Because of the IR surface selection rules, the RAIRS experiment is especially sensitive to tilt angle of the Pc chromophore. It has been shown that, when the plane of the Pc macrocycle in a thin film assembly is at 90° to the substrate in the RAIRS experiment, the δ_{Pc-H} bands completely disappear.[25] These transitions were clearly visible after transfer of our materials to the Au surface, which confirms the tilt of the Pc rings away from a perpendicular orientation.

The intensities in the ν_{Pc-O-C} and the δ_{Pc-H} bands, relative to the intensities in these bands in isotropic powders of these Pcs, provides estimates of these angles of inclination using data treatments developed by Debe.[27] For calculations of the tilt angle of the Pc with respect to the substrate plane, vibrations in and out of Pc macrocycle core were chosen to define a "molecular vibrational plane", $\nu_{(Pc-O-C,\ ip)}$ at 1204 and 1283 cm^{-1} in the plane of the Pc ring and $\delta_{(ring\ C-H,op)}$ at 745 cm^{-1}. This plane is therefore orthogonal to the real geometric plane of the Pc macrocycle. The orientation of the molecular vibrational plane is determined by formalisms which relate this plane to the surface coordinates via Euler angles. The Euler angles, ψ_{RAIRS} (an angle of rotation in the xy plane around z) and θ_{RAIRS} (an angle of rotation in the yz plane around x) are defined in relation to the molecular plane coordinates (x', y', z') and the surface coordinates (x, y, z) (Figure 9). The two sets of coordinates are related by a transformation matrix,

(25) Chesters, M. A.; Cook, M. J.; Gallivan, S. L.; Simmons, J. M.; Slater, D. A. *Thin Solid Films* **1992**, *210/211*, 538.
(26) Schmidt, V. S.; Reich, R. *Ber. Bunsen-Ges. Phys. Chem.* **1972**, *76*, 1202.
(27) Debe, M. K. *Appl. Surf. Sci.* **1982/1983**, *14*, 1.

$$\begin{pmatrix} x' \\ y' \\ z' \end{pmatrix} = \begin{pmatrix} \cos\psi_{\mathrm{RAIRS}} & \cos\theta_{\mathrm{RAIRS}}\sin\psi_{\mathrm{RAIRS}} & \sin\psi_{\mathrm{RAIRS}}\sin\theta_{\mathrm{RAIRS}} \\ -\sin\psi_{\mathrm{RAIRS}} & \cos\theta_{\mathrm{RAIRS}}\cos\psi_{\mathrm{RAIRS}} & \cos\psi_{\mathrm{RAIRS}}\sin\theta_{\mathrm{RAIRS}} \\ 0 & -\sin\theta_{\mathrm{RAIRS}} & \cos\theta_{\mathrm{RAIRS}} \end{pmatrix} \begin{pmatrix} x \\ y \\ z \end{pmatrix} \quad (4)$$

The ratio of the thin film in-plane and out-of-plane intensities ($I^{\mathrm{t}}_{\mathrm{i,i}}$ and $I^{\mathrm{t}}_{\mathrm{i,o}}$) with the bulk intensities ($I^{\mathrm{b}}_{\mathrm{i,i}}$ and $I^{\mathrm{b}}_{\mathrm{i,o}}$) are related to the Euler angles through the following relationships:

$$\frac{I^{\mathrm{t}}_{\mathrm{i,i}}}{I^{\mathrm{b}}_{\mathrm{i,i}}} = 3\cos^2\psi_{\mathrm{RAIRS}}\sin^2\theta_{\mathrm{RAIRS}}$$

and

$$\frac{I^{\mathrm{t}}_{\mathrm{i,o}}}{I^{\mathrm{b}}_{\mathrm{i,o}}} = 3\sin^2\psi_{\mathrm{RAIRS}}\sin^2\theta_{\mathrm{RAIRS}} \quad (5)$$

These ratios in the $\nu_{\mathrm{Pc-O-C}}$ and the $\delta_{\mathrm{Pc-H}}$ bands (Table 2) demonstrate that the Pc rings in our assemblies are inclined in two directions to the substrate normal (Figure 9), with average values of θ_{RAIRS} = ca. 15° (the twist of the Pc ring toward the reader, out of the plane of the paper) and ψ_{RAIRS} = ca. 31° (the tilt of the Pc ring away from the substrate normal, away from the reader. Looking down the Pc column axis, parallel to the substrate plane, we conclude that the projection of the molecular plane creates an elliptical shape for the center of the column. This elliptical projection can be compensated in a hexagonal close packed Pc columnar arrangement through distortion of the side chains, which would be necessary to help fill the void space between these side chains (not shown). The ratio of thin film to isotropic bulk intensities in the RAIRS data for the $\nu_{\mathrm{C-O-C}}$ stretch in the ethylene oxide side chains shows that these side chains are not as well ordered as the Pc rings within the columns and that the average angles of inclination of the side chain with respect to the Pc column director axis are smaller ca. 2° for the $CuPc(OC_2OBz)_8$ and ca. 9° for the $H_2Pc(OC_2OBz)_8$ films. Previous wide-angle X-ray scattering of fibers of these Pcs has shown broad reflections not associated with the Pc−Pc spacing, with lattice parameters which suggested a larger average spacing of the side chains than for the Pc rings (ca. 0.43 nm versus 0.34 nm) and significantly less order in these portions of the assembly.[14] These earlier observations are consistent with the column−column spacing suggested by the X-ray data above, which showed a column diameter smaller than expected if the side chains were fully extended, and the Pc rings were sitting completely perpendicular to the substrate plane (ca. 3.4−3.5 nm).

Conclusions

The combination of ethylene oxide and terminal benzyl groups creates a readily processable phthalocyanine assembly with excellent long-range order and anisotropy in electrical conductivity and visible and IR absorbance. This tendency toward formation of coherent and rigid Pc columns appears to have its origin in the expected Pc−Pc macrocycle interactions and in the added interactions between the terminal benzyl groups. We believe the added stability imparted to the bilayer Pc assembly, relative to other side chain modified Pcs, to be due to the accumulation of van der Waals contacts between these terminal benzyl groups. There is likely to be considerable side chain twisting in order to accommodate a maximum number of edge−edge and edge−cofacial interactions, both within the Pc columns and between these columns. While interdigitation of the columns cannot be completely ruled out, the images seen in STM/AFM studies, and that fact that these materials appear to retain their liquid crystallinity in macroscopic films or fibers, argues against this form of column−column interaction. Our AFM studies have also shown that the previously documented fiber forms of these materials, which arise during overcompression of the stable bilayer structures on the LB trough,[12] actually consist of tightly folded bilayer sheets, possessing hundreds of bilayer sheet thicknesses per fiber.[17] The rigidity imparted to the bilayer form of these materials, and the resultant efficiency of bilayer transfer, mechanical patterning, and change of column orientation from one dipping cycle to the next, suggests that these types of material properties should be sought in other discotic mesophase systems, and synthetic elaborations of the present Pc structure are underway.

In addition, while the conductivity of these assemblies can be increased through electrochemical doping, there is a clear need to improve the electrical contacts to these assemblies, to improve the coherence of individual columns even further, and to include different metals in the Pc core, to ascertain the maximum conductivity obtainable by small numbers of Pc columns.

Acknowledgment. The authors are grateful for the advice on AFM imaging given by Professor Srinivas Manne, Department of Physics, University of Arizona, for the preliminary exploration of the field-effect transistor properties of thin films of these materials by Dr. Zhenan Bao, Lucent Technologies, and for the X-ray scattering studies performed by Dr. Simon Bates, Kratos Analytical. Support for this research was provided by grants from the National Science Foundation (Chemistry and International Programs) (N.R.A.) and the Division of Materials Research (D.F.O.).

JA991498B